BIOCHEMISTRY
including biophysical chemistry & molecular biology

Article

pubs.acs.org/biochemistry

Membrane Interaction of Disease-Related Dynorphin A Variants

Johannes Björnerås, Astrid Gräslund, and Lena Mäler*

Department of Biochemistry and Biophysics, The Arrhenius Laboratory, Stockholm University, 10691 Stockholm, Sweden

ABSTRACT: The membrane interaction properties of two single-residue variants, R6W and L5S, of the 17-amino acid neuropeptide dynorphin A (DynA) were studied by circular dichroism (CD) and nuclear magnetic resonance (NMR) spectroscopy. Corresponding gene mutations have recently been discovered in humans and causatively linked to a neurodegenerative disorder. The peptides were investigated in buffer and in isotropic solutions of $q = 0.3$ bicelles with 1,2-dimyristoyl-*sn*-glycero-3-phosphocholine (DMPC) or DMPC (0.8) and 1,2-dimyristoyl-*sn*-glycero-3-phospho(1′-*rac*-glycerol) (DMPG) (0.2). The CD results and the NMR secondary chemical shifts show that R6W-DynA has a small α-helical fraction in buffer, which increases in the presence of bicelles, while L5S-DynA is mainly unstructured under all conditions studied here. R6W-DynA has an almost complete association with zwitterionic bicelles (~90%, as probed by NMR diffusion experiments), similar to the behavior of wtDynA, while L5S-DynA has a weaker association (~50%). For all peptides, the level of bicelle association is increased in negatively charged bicelles. The L5A-DynA peptide adopts a very shallow position in the headgroup region of the bicelle bilayer, as studied by paramagnetic spin relaxation enhancement experiments using paramagnetic probes. Similarly, the results show that R6W-DynA is more deeply buried in the bilayer, with only the C-terminal residues exposed to solvent, again more similar to the case of wild-type DynA. We suggest that the results presented here may explain the differences in cell toxicity of these disease-related neuropeptide variants.

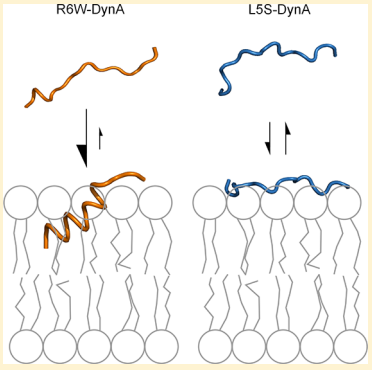

In the 1970s, a substance with distinct morphine-like properties was isolated from cow brain.[1] The substance was later identified as an endogenous opioid peptide and named dynorphin after its high potency in an assay using the contractions of guinea pig ileum.[2] Further research established that this powerful peptide exerted its opioid effects mainly through the κ subtype of the opioid receptors (KOR),[3−6] and that there are two types of dynorphins, dynorphin A (DynA) and dynorphin B (DynB), emanating from the same precursor protein, prodynorphin (PDYN).[7] These two central derivatives of prodynorphin are among the most basic naturally occurring peptides in the body (Table 1).[8] DynA, the most studied member of the dynorphin family of neuropeptides, is mainly connected with pain regulation and analgesic effects through interactions with the opioid receptors,[9,10] but also with higher-level physiological processes such as addiction and reward,[11,12] as well as various psychiatric disorders.[13]

Table 1. Sequences of the DynA Peptides and Free Energies of Transfer between Water and POPC

	sequence	ΔG_{total}[a] (kcal/mol)	ΔG_{Res1-9}[a] (kcal/mol)
wild-type DynA	YGGFL RRIRP KLKWD NQ	1.76	−0.49
R6W-DynA	YGGFL WRIRP KLKWD NQ	−0.90	−3.15
L5S-DynA	YGGFS RRIRP KLKWD NQ	2.45	0.2

[a]Based on the Wimley−White scale.[71]

In addition to the opioid system, DynA has been implicated in several other signaling pathways, not involving the opioid receptors, is connected to a wide variety of physiological effects. These so-called non-opiate effects, most often studied in cellular systems, mice or rats, include paralysis,[14] changes in the motor system,[15] and apoptosis of neural cells.[16] Functions related to direct membrane interactions have also been suggested, including translocation into cells[17] and the formation of pores that have been suggested to play a role in the influx of calcium into cells.[18] DynA has further been suggested to disrupt phospholipid bilayers by lysis and bilayer fusion and to induce formation of vesicles in ordered bilayers.[19] Hence, it appears that DynA has a wide range of disruptive effects on bilayer integrity.

Since the discovery of the dynorphins, a large number of research groups have used truncations, mutations, chemical modifications, and various forms of cyclization of the peptides, in particular DynA, to map out the physicochemical and structural properties needed for potent and selective KOR agonist and antagonist effects.[20−36] Partly, this research has been driven by the desire to develop analgesic compounds matching morphine, the "gold standard", but without its serious adverse side effects, such as addiction. The results of this research include a number of synthetic nonpeptide ligands, one of which was recently used in the successful crystallization of the KOR and the determination of its structure.[37]

Received: April 4, 2013
Revised: May 24, 2013
Published: May 24, 2013

   dx.doi.org/10.1021/bi4004205 | *Biochemistry* 2013, 52, 4157−4167

In sharp contrast to the abundance of synthetically modified DynA peptides and analogues, no naturally occurring variants were known until recently, when mutations in the gene encoding PDYN were identified and shown to be the cause of a particular form of the human neurodegenerative disorder spinocerebellar ataxia 23 (SCA23).[38] Shortly thereafter, another set of mutations was found in the PDYN gene.[39] Of these identified mutations, three belong to the DynA-coding sequence and correspond to peptide variants R6W, L5S, and R9C. Transfection of cells with cDNA of the different mutants resulted in 10−18-fold elevated levels of processed R6W-DynA and L5S-DynA, compared to that of the wild type (wtDynA), while the R9C-DynA variant was processed to yield only a fraction of the amounts of wtDynA.[38] Cell toxicity studies showed negligible effects of L5S-DynA, while R6W-DynA caused a 3-fold increase in the level of induced cell death compared to that of wtDynA.[38] A biophysical study showed that L5S-DynA did not cause significant membrane perturbations, whereas R6W-DynA induced a significant amount of leakage in unilamellar liposomes.[40] Hence, it appears that of the known mutations linked to SCA, two result in appreciable levels of processed DynA peptides, and these two variants, R6W-DynA and L5S-DynA, have markedly different effects on membranes.

To improve our understanding of the molecular mechanisms behind the direct membrane interaction of R6W-DynA and L5S-DynA, we have in this report investigated their bilayer-interacting properties using circular dichroism (CD) and nuclear magnetic resonance (NMR) spectroscopy. Direct membrane interactions are believed to have effects on both receptor binding through preadsorption of the ligand to the membrane, possibly imposing structural constraints of the peptide,[41] and on direct membrane penetration.[17] Interactions between dynorphins and membranes or membrane mimetic media have been studied previously.[18,42−45] Here we use fast-tumbling bicelles,[46,47] a lipid bilayer system amenable to solution state NMR, to study the structural properties of the variant DynA peptides as well as overall association to and orientation in the bilayer. Fast-tumbling bicelles with low q values have relatively small sizes for which reasonable spectra of bound peptides and proteins can be obtained with conventional NMR methods. To study the effect of membrane surface charge on the interaction, we replaced 20% of DMPC with DMPG, which also mimics the anionic content of, for example, nervous cells.[48] Our results demonstrate that the two variant peptides have very different membrane interacting properties, which in turn may be related to the their different toxicity and membrane-disrupting properties.

MATERIALS AND METHODS

Materials. Synthetic peptides corresponding to the sequence of wtDynA, and the R6W-DynA and L5S-DynA variants, were obtained from PolyPeptide Group (Strasbourg, France) and used without further purification. Both unlabeled 1,2-dihexanoyl-*sn*-glycero-3-phosphocholine (DHPC) and DHPC with deuterated acyl chains (d_{22}-DHPC) were used as the short chain phospholipid in the preparation of phospholipid bicelles. 1,2-Dimyristoyl-*sn*-glycero-3-phosphocholine (DMPC or d_{54}-DMPC) and 1,2-dimyristoyl-*sn*-glycero-3-phospho(1′-*rac*-glycerol) (DMPG or d_{54}-DMPG) were used to produce the bilayer in the phospholipid bicelles. 1-Palmitoyl-2-stearoyl(5-doxyl)-*sn*-glycero-3-phosphocholine (5-DOXYL-POPC) was used for paramagnetic relaxation enhancement experiments. All lipids were obtained from Avanti Polar Lipids (Alabaster, AL).

Preparation of Bicelles. Fast-tumbling DMPC/DHPC bicelles with a q of 0.3 [q is the molar ratio of lipids and detergents, e.g., q = [DMPC]/[DHPC] or q = ([DMPC] + [DMPG])/[DHPC]] were produced by mixing DMPC (powder) with buffer and adding a suitable amount of a 1 M aqueous solution of DHPC to the mixture to obtain a total lipid ([DMPC] + [DHPC]) concentration of 150 mM as described previously.[49] This mixture was vortexed several times until a clear nonviscous solution was obtained. Partly negatively charged bicelles containing DMPC and DMPG were produced as described above, but with 20 mol % of the DMPC replaced with DMPG (e.g., [80% DMPC + 20% DMPG]/DHPC). For diffusion measurements, d_{22}-DHPC was used.

Circular Dichroism Spectroscopy. CD spectra were recorded on a Chirascan circular dichroism spectrometer (Applied Photophysics, Surrey, United Kingdom)) with a 0.1 mm cuvette at 37 °C. The temperature was maintained with a TC 125 temperature control unit. Spectra were recorded with 10 scans, with a bandwidth of 1 nm and a speed of 240 nm/min, using 0.5 nm steps. Measurements were taken with 0.25 mM peptide, at pH 5.7, in 50 mM sodium phosphate buffer only, and in buffered solutions of DMPC/DHPC or DMPC/DMPG/DHPC bicelles. The total lipid concentration was 150 mM for all bicelle samples, giving a peptide:bicelle millimolar ratio of ∼1:2, assuming ideal bicelle morphology. Background spectra of bicelles only were recorded and subtracted from the peptide spectra. The spectra were processed with the Chirascan software and analyzed MATLAB version 7.0 (http://www.mathworks.com). Estimates of secondary structure content were made with the software on the K2D3 analysis server.[50]

NMR Spectroscopy. NMR samples were prepared using a peptide concentration of approximately 1 mM, and a sodium phosphate buffer concentration of 50 mM, in a 150 mM DMPC/DHPC or DMPC/DMPG/DHPC solution using a total volume of 500 μL, including 10% D_2O for field-frequency lock stabilization. If needed, the pH was adjusted to 5.7 with 0.1 M HCl and/or 0.1 M NaOH. All two-dimensional (2D) measurements were taken at 37 °C, while the diffusion experiments were conducted at 25 °C. All spectra were processed with NMRPipe[51] and analyzed with Sparky version 3.114 (http://www.cgl.ucsf.edu/home/sparky).[52]

Homonuclear 2D TOCSY and NOESY spectra were recorded for assignment purposes using a Bruker Avance NMR spectrometer (Bruker Biospin, Fällanden, Switzerland), equipped with a cryo-probe, operating at a field strength of 11.74 T (500 MHz ^{1}H frequency). The spectral width was 6000 Hz in both dimensions, and the spectra were collected with 8192 data points in the ω_2 dimension and 450−500 in the ω_1 dimension; 32−48 scans were taken. Before Fourier transformation, the data were zero filled to 16384 data points in ω_2 and 2048 in ω_1. The TOCSY spectra were recorded with an MLEV spin-lock using mixing times of 30−80 ms, and the NOESY spectra were recorded with mixing times of 200−300 ms using a recycle delay of 2 s for the TOCSY and NOESY spectra. Chemical shifts were referenced to the internal chemical shifts of the lipids. The ^{1}H backbone chemical shift assignments of R6W-DynA and L5S-DynA in buffer, in a DMPC/DHPC solution, and in a DMPC/DMPG/DHPC solution have been deposited with the Biological Magnetic Resonance Bank (BMRB, http://www.bmrb.wisc.edu/) as entries 19140 and 19141, respectively.

NMR paramagnetic relaxation enhancement (PRE) experiments using two types of paramagnetic probes were performed to probe the location of specific residues within the bilayer. 1-Palmitoyl-2-stearoyl(5-doxyl)-*sn*-glycero-3-phosphocholine lipids with a free radical DOXYL group attached to the stearoyl chain C5 position (5-DOXYL-POPC) were introduced into the bicelles to probe positions deep in the lipid bilayer,[53] while Mn^{2+} ions, added in the form of $MnCl_2$, were used as complementary probes for the bilayer surface region. The 5-DOXYL-POPC was integrated into bicelles by adding 3 μL of a 50 mM solution in chloroform to 500 μL of 150 mM bicelle samples to reach a final spin label concentration of 0.3 mM. Mn^{2+} ions were added to the samples as small amounts of an aqueous solution of $MnCl_2$ (100 mM) to a final concentration of 0.5 mM. Two TOCSY spectra with mixing times of 40 ms were recorded using the same parameters as described above, one without a spin-label and one with an added spin-label. The paramagnetic relaxation enhancement factors were evaluated by examining the remaining amplitudes of $^1H^N-^1H^\alpha$ cross-peaks and taking the ratio between the amplitude in a spectrum without the label and the remaining amplitude in a spectrum with the label present. If the largest remaining amplitude exceeded the corresponding amplitude in the spectrum from the sample without a spin-label, this ratio was normalized to unity and this normalization factor was used for all ratios.

Translational diffusion measurements were taken on a Bruker Avance spectrometer (Bruker Biospin), equipped with a triple-resonance probe head, operating at 14.1 T (600 MHz ^1H frequency) at 25 °C for samples dissolved in D_2O. Measurements were performed for samples containing 1 mM peptide in 50 mM phosphate buffer and in a DMPC/DHPC or DMPC/DMPG/DHPC solution. A standard sample consisting of 0.01% H_2O in D_2O and 1 mg/mL $GdCl_3$ was used for gradient calibration at 25 °C. Translational diffusion coefficients were measured using a modified Stejskal-Tanner spin−echo experiment[54−56] with a fixed diffusion time of 100 ms for peptides in buffer, while for peptide and DMPC in bicelle solutions, the reported diffusion coefficients are averages from measurements with diffusion delays of 250 and 500 ms, respectively. A gradient length, δ, of 4 ms was used for all experiments, and the square of the gradient strength increased linearly over 16 steps from 5 to 95% of the maximal gradient strength (55 G/cm). A total of 16−64 scans were recorded for each gradient strength using 16K data points. The recycle delay was set to 5 s. The attenuation of the signal as a function of increasing gradient strength was measured and analyzed using the Stejskal−Tanner equation.[55] All diffusion values reported are the average values from two separate experiments. To measure the translational diffusion of DMPC (or DMPG), the ^1H resonance at 0.715 corresponding to the DMPC/DMPG acyl chain methyl peak was used. For the peptides, the signal intensities of the aromatic resonances were used. The measured translational diffusion rate of residual HDO in the samples was used together with the diffusion coefficient of pure water to estimate, and compensate for, viscosity differences in the different samples.[57]

RESULTS

Overall Conformation of R6W-DynA and L5S-DynA. To study the bilayer-induced structural differences between the peptides, we used small (q = 0.3), fast-tumbling bicelles to mimic a bilayer. We chose these bicelles because previous NMR studies of wtDynA were conducted in such bicelles.[44] Studies of bicelles with a q of >0.5 have indicated that low-q value bicelles may be described as mixed micelles.[58,59] On the other hand, Glover et al. have shown that the morphology of bicelles persists also at low q values,[46] with a separation of DMPC and DHPC as evidenced by ^{31}P NMR spectroscopy. When separate, the two components had identical chemical shifts, while in q = 0.5 bicelles, distinct resonances for the two components were observed, indicating different environments. Likewise, Chou et al. demonstrated that the chemical shifts, and thus structural properties, for the HIV-1 Env peptide did not change in bicelles with q values of >0.25, but that the spectral properties differed from those of micelles.[60] Spin relaxation and translational diffusion experiments have also been used to model the morphology of q = 0.25−0.5 bicelles.[61] Hence, we conclude that our bicelles should be reasonable bilayer models, but perhaps somewhat different from higher-q value mixtures.

CD spectra were recorded for the DynA variants in three solvents: buffer or buffered q = 0.3 DMPC/DHPC and DMPC/DMPG/DHPC solutions (Figure 1). Previous CD studies of wtDynA in the same bicelle environments[44] showed virtually no difference compared to the results in POPC and POPC/POPG unilamellar vesicles, indicating that the structure of DynA is not dependent on the specific type of membrane mimetic in this case.[17] In buffer, the R6W variant appears to be mainly unstructured, but the spectral minimum at 202 nm, together with a small but visible shoulder at 220 nm, suggests a small fraction of α-helix (Figure 1a). This helical fraction increases markedly in the presence of both bicelle solutions, as evidenced by the two minima becoming more visible, and shifting toward 208 and 222 nm. Estimating the helical content

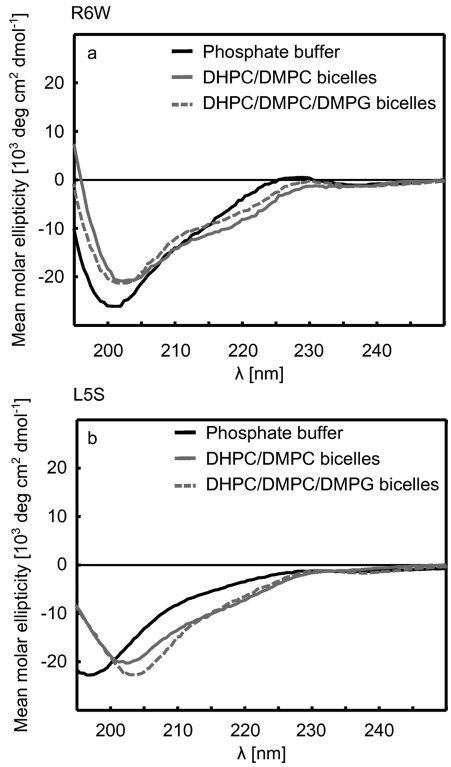

Figure 1. Circular dichroism spectra of R6W-DynA (a) and L5S-DynA (b). Spectra were recorded in 50 mM sodium phosphate buffer (pH 5.7) (black solid line), in a DMPC/DHPC bicelle solution (gray solid line), and in a DMPC/DMPG/DHPC bicelle solution (gray dashed line).

dx.doi.org/10.1021/bi4004205 | *Biochemistry* 2013, 52, 4157−4167

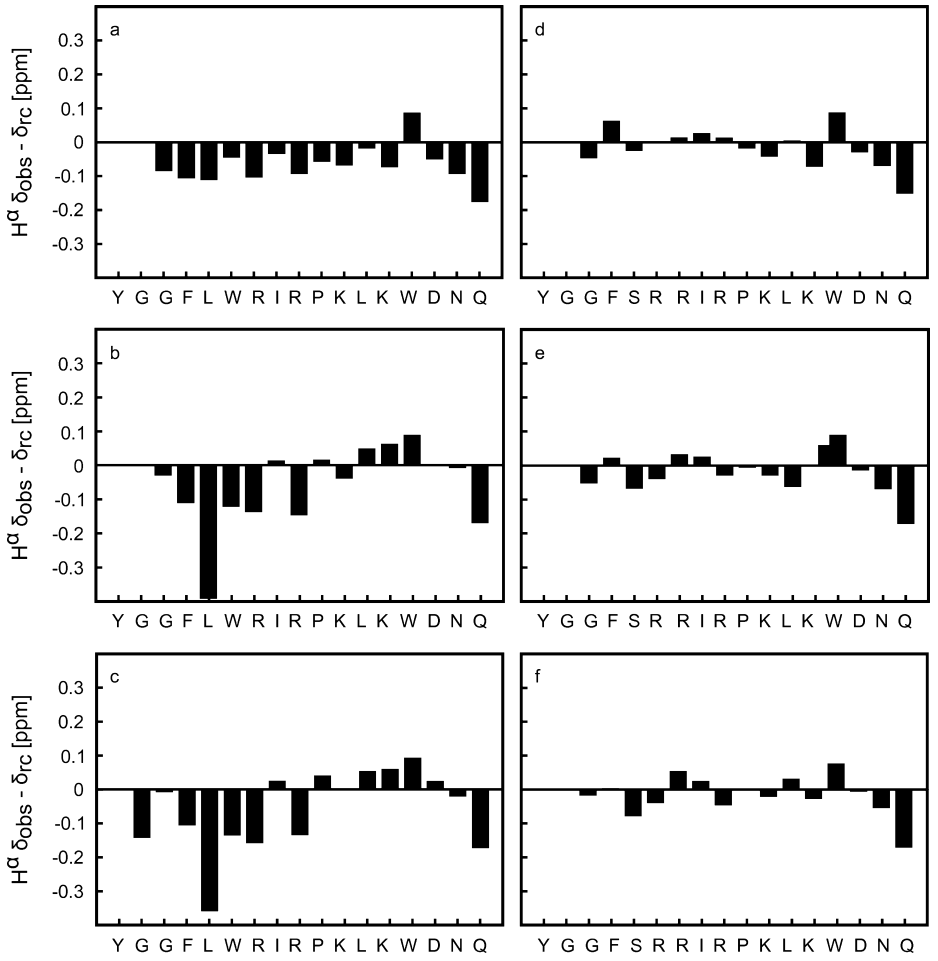

Figure 2. Differences between observed and random coil[57] NMR H^{α} chemical shifts for the two variants. (a–c) Results for R6W-DynA in 50 mM sodium phosphate buffer (pH 5.7) (a), in a DMPC/DHPC bicelle solution (b), and in an (80% DMPC + 20% DMPG)/DHPC bicelle solution (c). (d–f) Results for L5S-DynA in 50 mM sodium phosphate buffer (pH 5.7) (d), in a DMPC/DHPC bicelle solution (e), and in a DMPC/DMPG/DHPC bicelle solution (f).

in R6W-DynA from a set of theoretically derived reference spectra as implemented in K2D3[51] reveals that the peptide adopts approximately 15% helical structure in buffer and that the helical content increases to 30% in either of the bicelle solutions.

^{1}H NMR spectra were recorded for the R6W-DynA peptide in buffer as well as neutral and negatively charged q = 0.3 bicelles, and the resonances were assigned. The differences between the observed H^{α} chemical shifts for R6W-DynA and random coil shifts as reported by Wishart et al.[62] indicate a weak tendency toward α-helix structure in buffer (Figure 2a) and an increased fraction of helical structure in the presence of either neutral (Figure 2b) or charged (Figure 2c) bicelles. No significant differences in the structural induction comparing the DMPC/DHPC with DMPC/DMPG/DHPC bicelles were observed.

Overall, the peaks in the 2D spectra are broadened in the presence of both types of bicelles, as compared to those in buffer, indicating association or exchange broadening (Figure 3). An analysis of the NOESY data for R6W-DynA showed no cross-peaks indicative of helical structure in aqueous solvent, but in both bicelle environments the presence of fairly strong sequential H^N–H^N cross-peaks starting from Phe4 and ranging all the way to Asn16 (with the obvious exception of Pro10) indicated a structured peptide (Figure 3a). No unambiguous H^{α}–$H^N(i, i + 3)$ or H^{α}–$H^N(i, i + 4)$ could, however, be found, partly because of the unfortunate overlap between several residues. In general, very few cross-peaks were seen in the NOESY spectrum, supporting the CD results. Together, these results indicate a rather weak structure induction. In agreement with the CD data, no significant differences were observed between the DMPC/DHPC and DMPC/DMPG/DHPC bicelle-induced effects.

L5S-DynA shows a similar pattern, but the extent is much lower. The CD spectrum in buffer (Figure 1b) indicates that the peptide is mainly in a random coil structure, and while there are indications of induction of more ordered structure in the CD spectra upon addition of bicelles, this is not as pronounced as for R6W-DynA (an increase from 5% α-helical structure in buffer to a maximum of 9% in the bicelle solutions). From the ^{1}H NMR spectra, the H^{α} secondary shifts indicate a disordered polypeptide in all three solvents (Figure 2d–f). Compared to R6W-DynA, L5S-DynA shows even fewer cross-peaks in the NOESY spectrum, again in agreement with the CD data (Figure 3b). The scarcity of NOE cross-peaks (Figure 3b) supports the conclusion that L5S-DynA is much less structured than R6W-DynA. For L5S-DynA, no H^{α}–H^N cross-peaks, except for intraresidue and sequential ones, were observed. Moreover, H^N–H^N NOEs were observed for only residues Arg7 and Ile8, Ile8 and Arg9, Leu12 and Lys13, and Asp15 and

dx.doi.org/10.1021/bi4004205 | *Biochemistry* 2013, 52, 4157–4167

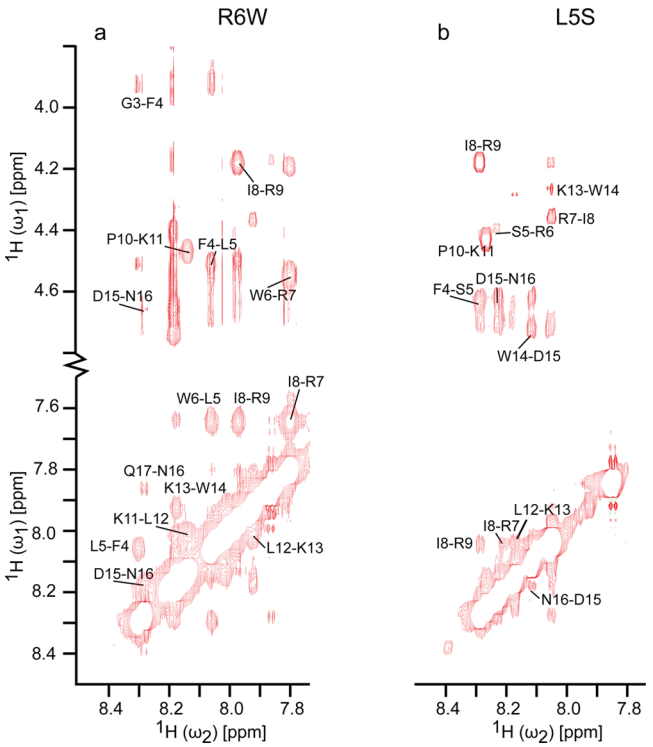

Figure 3. Details of 500 MHz NOESY spectra for 1 mM R6W-DynA (a) and 1 mM L5S-DynA (b) in 150 mM, q = 0.5 DMPC/DHPC bicelles. The sequential assignments are indicated.

Asn16. Again, no differences were observed between the two bicelle systems.

We conclude that weak structural features are present in R6W-DynA in buffer, and that these are enhanced by interaction with the bicelles, while much less structural induction is observed in L5S-DynA. Furthermore, negatively charged lipids do not appear to be important for the structure of either of the two DynA variants.

Association with Bicelles. NMR translational diffusion experiments provide information about the degree of association between entities in a solution and have been used here to study the bicelle-bound fraction of peptides (at equilibrium) for the different DynA variants. The diffusion rates of wtDynA, R6W-DynA, and L5S-DynA were measured in buffer and in bicelle solution, and together with the measured bicelle diffusion rate, the fraction of peptides bound to bicelles was estimated through eq 1, under the approximation that the peptide–bicelle complex diffuses with the same rate as an empty bicelle. The fraction of bicelle-bound peptide, p_{bound}, may thus be estimated from

$$p_{bound} = \frac{D_{pep,bicelle} - D_{pep,buffer}}{D_{bicelle} - D_{pep,buffer}} \quad (1)$$

where p_{bound} is the fraction of bicelle-bound peptide, $D_{pep,bicelle}$ is the diffusion rate of the peptide in the presence of bicelles, $D_{pep,buffer}$ is the diffusion rate of the peptide in buffer, and $D_{bicelle}$ is the diffusion rate of the bicelles, as determined by the diffusion of DMPC. Translational diffusion data for wtDynA and the two variants in DMPC/DHPC and DMPC/DHPG/DHPC bicelles are summarized in Table 2. The size of the bicelles can be related to an effective hydrodynamic radius through the Stokes–Einstein equation. Using this, and correcting for the viscosity differences between light and heavy water, we find that the bicelles with associated peptides have a hydrodynamic radius of around 3 nm, in agreement with similar bicelle systems investigated previously.[61]

Table 2. Diffusion Coefficients for the DynA Variants and Bicelles in Buffered D_2O

	D_{pep} ($\times 10^{-10}$ m^2/s)	$D_{bicelle}$ ($\times 10^{-10}$ m^2/s]	bicelle association (%)[a]
wtDynA, buffer	1.62 ± 0.01		
wtDynA, DMPC/DHPC	0.80 ± 0.04	0.67 ± 0.03	86
wtDynA, DMPC/DMPG/DHPC	0.72 ± 0.02	0.69 ± 0.01	97
R6W-DynA, buffer	1.65 ± 0.07		
R6W-DynA, DMPC/DHPC	0.74 ± 0.07	0.63 ± 0.03	89
R6W-DynA, DMPC/DMPG/DHPC	0.65 ± 0.01	0.63 ± 0.01	98
L5S-DynA, buffer	1.69 ± 0.04		
L5S-DynA, DMPC/DHPC	1.21 ± 0.05	0.67 ± 0.01	47
L5S-DynA, DMPC/DMPG/DHPC	0.87 ± 0.02	0.65 ± 0.01	79

[a]Estimated using eq 1.

Both wtDynA and R6W-DynA associate to a very high degree with DMPC/DHPC bicelles, with estimated bound populations of 86 and 89%, respectively (Table 2), and the degree of association is almost 100% in DMPC/DMPG/DHPC bicelles. For the L5S-DynA variant, on the other hand, only approximately half of the peptides (47%) associated with DMPC/DHPC bicelles, while a larger fraction associated with the DMPC/DMPG/DHPC bicelles (79%), indicating a very different type of membrane interaction than what is observed for R6W-DynA. The higher degree of association with anionic lipids is expected because all variants carry a net positive charge (Table 1). Although the degree of association increases when negatively charged lipids are added to the bicelles, this increase in the level of association is not accompanied by a structural change in the peptides. One may also note that a larger fraction of L5S-DynA remains in solution as compared to wtDynA and R6W-DynA also in the partly anionic bicelles.

Effects of Mutation As Determined via Comparison with wtDynA. The chemical shifts of backbone protons of wtDynA in bicelle environments have been reported previously.[44] The effects of the point mutations in the variants, R6W-DynA and L5S-DynA, were studied here by comparison with the corresponding shifts of wtDynA.[63] For R6W-DynA, the H^N shift differences compared to those of wtDynA in buffer are overall small (<0.05 ppm), with the exception of residues Leu5, Ile8, and Arg9, as one can see in Figure 4. Leu5 is adjacent to the mutation site, while Arg9 and Ile8, which exhibit the largest changes in chemical shift (almost 0.3 ppm), are not. The H^α shift changes are much smaller, with the largest deviations close to the mutation (Phe4 and Arg7).

In the presence of DMPC/DHPC bicelles, residues Gly3, Phe4, and Leu5 in R6W-DynA have significantly lower H^N chemical shifts than wtDynA, indicating either a structural difference, a location in a different environment,[64] or both. The sequence of Leu12, Lys13, and Trp14 near the C-terminus, on the other hand, shows the largest positive shift differences compared to those of wtDynA, indicating a higher degree of hydration.[64] The three remaining residues at the C-terminus have very small chemical shift differences compared to those of wtDynA, indicating that the C-termini experience similar

dx.doi.org/10.1021/bi4004205 | Biochemistry 2013, 52, 4157–4167

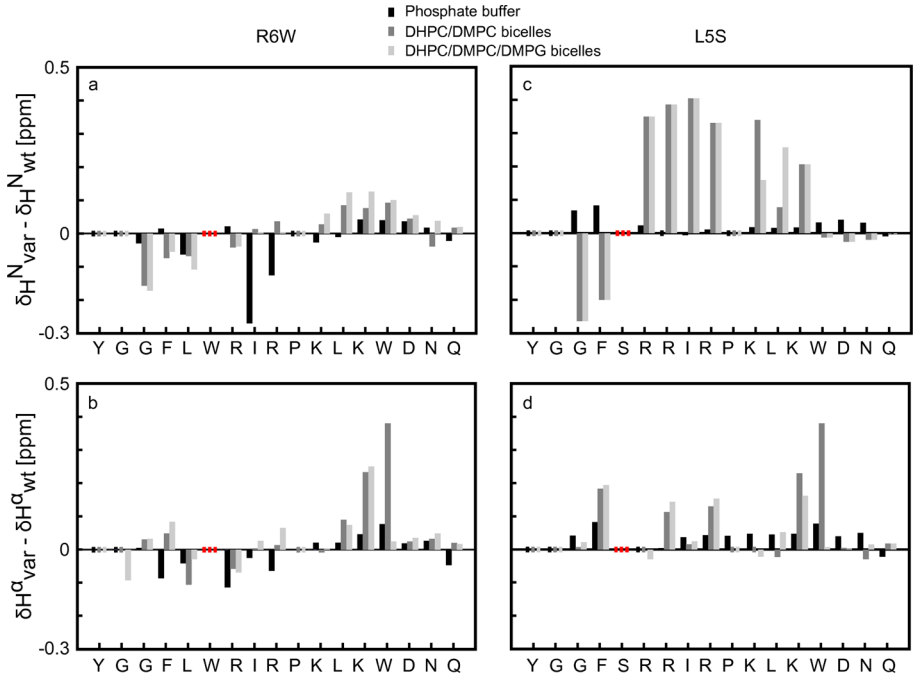

Figure 4. Comparison of chemical shifts between the DynA variants and wtDynA. Chemical shift differences between R6W-DynA and wtDynA[44] for $^1H^N$ (a) and $^1H^\alpha$ (b) atoms, and between L5S-DynA and wtDynA[44] for $^1H^N$ (c) and $^1H^\alpha$ (d) atoms. Black bars indicate data for 50 mM sodium phosphate buffer (pH 5.7), dark gray bars data for a DMPC/DHPC bicelle solution, and light gray bars data for DMPC/DMPG/DHPC bicelles. Red color indicates the site of mutation.

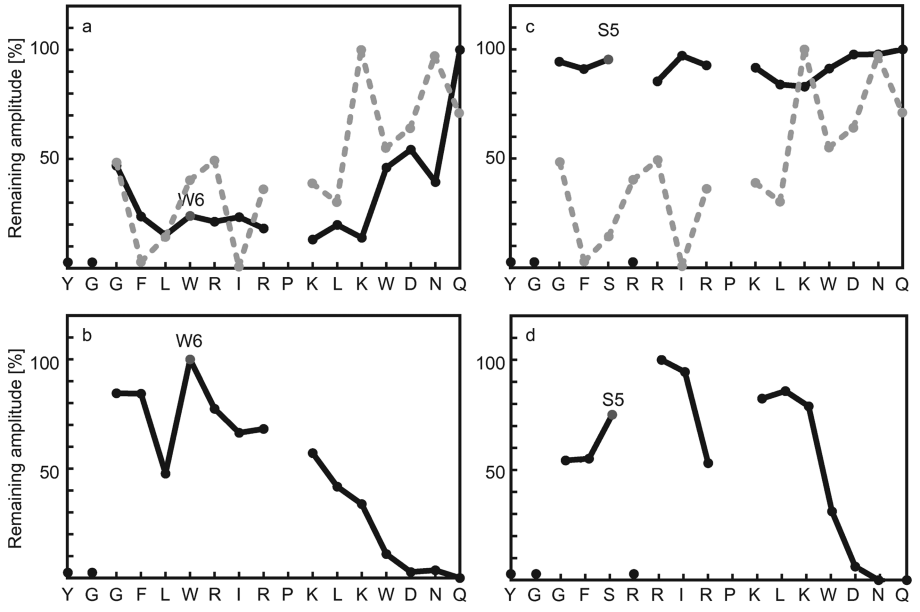

Figure 5. Effect of paramagnetic probes on cross-peaks in 500 MHz TOCSY spectra. Solid black lines show the remaining H^N–H^α TOCSY cross-peak amplitude for R6W-DynA after addition of 5-DOXYL-POPC (a) and $MnCl_2$ (b) and for L5S-DynA after addition of 5-DOXYL-POPC (c) and $MnCl_2$ (d). Dashed gray lines indicate previously published data for the effect of 5-DOXYL-POPC on wtDynA.[44] The residues for which no data could be obtained (missing resonances) are indicated by circles at the bottom of the graphs.

chemical environments in the two peptides. A comparison of the H^α shifts in R6W-DynA and wtDynA in the two bicelle environments (Figure 4a) reveals significant shift differences for Leu12, Lys13, and Trp14, for which the chemical shift values are larger in the variant, indicating less helical structure than in wtDynA. The results for the two types of bicelles are overall very similar, with the most notable exception being the H^α shift of Trp14, where the presence of DMPC/DHPC shifts this peak by almost 0.5 ppm compared to that of the wild type, while the resonance is almost unaffected in the presence of DMPC/DMPG/DHPC bicelles.

For L5S-DynA, the ^1H NMR chemical shift differences follow a clearly different pattern in which the peptide in buffer appears very similar to wtDynA, with only small changes in both H^N and H^α chemical shifts. Comparing the shifts for L5S-DynA with wtDynA in buffer is not straightforward, because only a fraction of L5S-DynA is bound to bicelles (50% to DMPC and 80% to DMPC/DMPG), while almost all of

dx.doi.org/10.1021/bi4004205 | *Biochemistry* 2013, 52, 4157–4167

wtDynA is associated with either of the two bicelles. Nevertheless, the amide proton resonances of the midsequence of the peptide, from Arg6 to Lys13, have significantly higher chemical shift values in L5S-DynA than in wtDynA. The differences range from 0.1 to 0.4 ppm. In contrast, the amide proton chemical shifts of Gly3 and Phe4 are smaller by approximately 0.2 ppm than for the wtDynA. As for R6W-DynA, the shift differences between L5S-DynA and wtDynA are very similar in the two bicelle solutions. Together, the results indicate that R6W-DynA is overall more similar to wtDynA than to L5S-DynA in terms of membrane interacting properties. Although the degree of association with DMPC compared to that with DMPC/DMPG bicelles is different for both variants, it appears that the shift differences are not affected by this association.

Positioning of R6W-DynA and L5S-DynA in Bicelles. To further investigate the environment of the two DynA variants in bicelles, two types of paramagnetic relaxation enhancement agents were used to address the question of the position of the backbone amides of two peptides in the lipid bilayer. Relaxation enhancement data for the two peptides using 5-DOXYL-POPC and Mn^{2+} are shown in Figure 5. Previous data for the effect of 5-DOXYL-POPC on wtDynA are also indicated in panels a and c of Figure 5. The influence of these probes on the relaxation of the amide protons was monitored by recording changes in H^N-H^α cross-peak amplitudes in TOCSY spectra. Previously published results for wtDynA[44] suggest that the N-terminus of this peptide dips down into the bilayer, while the C-terminal residues reside on the outside of the bicelles. These results also show some periodicity in the remaining cross-peak amplitudes along the sequence, an observation that has previously been made for amphipatic helices.[65] A similarly tilted orientation of wtDynA in a lipid bilayer has been shown in another study, based on molecular modeling results.[66]

For R6W-DynA, the relaxation of residues in the central region is strongly affected by the 5-DOXYL-POPC, with only around 20% of the signal amplitude remaining for all residues between Phe4 and Lys13, after the addition of the spin-label. Gly3 is less affected, with around half the amplitude remaining. The C-terminal residues are influenced by 5-DOXYL-POPC to a lower degree, with the terminal Gln17 virtually unaffected by the probe. Because of the extensive dynamics of the lipid chains, and hence also the DOXYL moiety, quantitative distances are difficult to obtain,[53] but a qualitative description is that the middle segment of the peptide, starting with Phe4, is buried in the bicelle close to the probe at position 5 of the acyl chain, while the most plausible interpretation for the C-terminus is that it is positioned either in the lipid headgroup region or outside of the bicelle. Mn^{2+} ions were added to examine the possibility of residues residing outside or close to the phosphates of the headgroup region in the bilayer. This resulted in an almost complete disappearance of the cross-peaks of the four C-terminal residues after addition of the probe, showing that the C-terminal part of the peptide is located within the headgroup region or outside of the bicelle. The effects on the amide protons gradually decrease toward the N-terminus, which appears much more protected from the Mn^{2+} ions, in agreement with the 5-DOXYL-POPC results. For some residues (Leu5, Leu12, and Lys13), similar effects of the 5-DOXYL and Mn^{2+} probes are observed. The most likely explanation for this is that the peptide has a high degree of flexibility, and that these residues, located in the interface between the interior of the bicelle and the headgroup region, can be affected by both probes. We conclude that a large part of R6W-DynA adopts a position within or at the headgroup region of the bicelle, with the C-terminal residues on the outside, and the Phe4-Lys13 sequence on the inside of the headgroup region.

For the L5S variant, a very different picture emerges from the experiments with the paramagnetic probes. Here there is virtually no effect of the lipid chain DOXYL group on any amide proton along the peptide backbone, with at least 80% cross-peak amplitude remaining for all residues after addition of the probe. Correspondingly, the Mn^{2+} ions have stronger effects that are, however, not uniform along the backbone. As for R6W-DynA, the signals for the three C-terminal residues almost completely disappear upon addition of Mn^{2+}, indicating full accessibility for the ions, while a much weaker effect is observed for Arg7, Ile8, Lys11, Leu12, and Lys13. One should keep in mind that only around 50% of the peptide is on average bound to zwitterionic bicelles, and that Mn^{2+} should have different effects on the free peptide compared to the bound peptide. Hence, the residues for which Mn^{2+} has a larger effect most likely interact with the surface of the bicelle, although the results do not provide conclusive evidence of the location of the peptide when in contact with the bicelle. In summary, these data indicate, together with the translational diffusion results, that the peptide is rather loosely associated with the bicelles, residing somewhere in the surface layer, but with the central part of the sequence not being fully accessible to either of the two probes.

DISCUSSION

In this work, we have studied the differences in the membrane interaction properties of two variants of the neuropeptide dynorphin A: R6W-DynA and L5S-DynA. These variants have recently been linked to the neurodegenerative disorder SCA23 and have also been shown to have drastically different cell toxicity properties,[38] as well as the capacity to induce leakage from large unilamellar vesicles.[40] From those data, it was concluded that R6W-DynA is more toxic to cells and that it induces approximately as much leakage in model liposome systems as does wtDynA, while L5S is much less harmful to cells and has virtually no membrane-perturbing effects in the leakage assay. In this study, the molecular determinants for membrane interactions of the variants have been compared to each other as well as to those of the wtDynA peptide whose membrane interaction properties have been reported previously.[44]

The results show that R6W-DynA is partly structured, showing helical character in phosphate buffer and even more helicity in a solution of fast-tumbling bicelles. This is also reflected in the NMR secondary chemical shifts, where in buffer the H^α shifts suggest a slight helical tendency for the N-terminal half of the peptide, a tendency that is reinforced in the presence of neutral or negatively charged bicelles. Compared to wtDynA, this variant appears to be slightly more structured on the whole, but at the same time, the C-terminus is slightly less structured. The L5S variant, on the other hand, has NMR chemical shifts very close to random coil values, while CD measurements suggest a small fraction of ordered structure elements. For both variants, as well as for wtDynA,[44] the structure has virtually no dependence on lipid charge, and although the degree of association with bicelles is modulated by anionic lipids for both

dx.doi.org/10.1021/bi4004205 | Biochemistry 2013, 52, 4157−4167

peptides, this indicates that electrostatics play only a small role in the membrane-induced structural rearrangements.

A combination of paramagnetic relaxation enhancement and analysis of chemical shifts shows that R6W-DynA inserts its N-terminal sequence into the lipid chain core of the bicelles while the C-terminus is on the outside, accessible to the solvent. Compared to that of wtDynA, the N-terminus is slightly more structured and inserts deeper with the N-terminal half of the sequence into the bilayer (Figure 6). Although wtDynA has the same affinity for the bicelles, the Arg6 to Trp mutation makes the peptide more prone to deeper insertion into the bilayer, as evidenced by the paramagnetic probe experiments. Moreover, the inserted Trp6 residue is less affected by Mn^{2+} ions in the paramagnetic relaxation enhancement experiments than its adjacent residues, despite showing a similar proximity to the DOXYL probe. This is consistent with the idea that Trp side chains have a more well-defined position as an anchor between the hydrophobic region of the lipid chains and the more polar environment of the phosphate headgroups when interacting with a bilayer.[67,68] In a solid state NMR study, Uezono et al. reported that the N-terminus of DynA inserted into a bilayer with a helical structure, while the remaining part of the sequence was largely random coil and located at the bilayer surface.[69] They reported a helical structure for Gly2−Leu5 and that this part of the peptide inserted in the bilayer, in agreement with solution state NMR of wtDynA in fast-tumbling bicelles.[44] Compared to wtDynA, it then appears that a longer sequence of R6W-DynA is inserted into the bicelle.

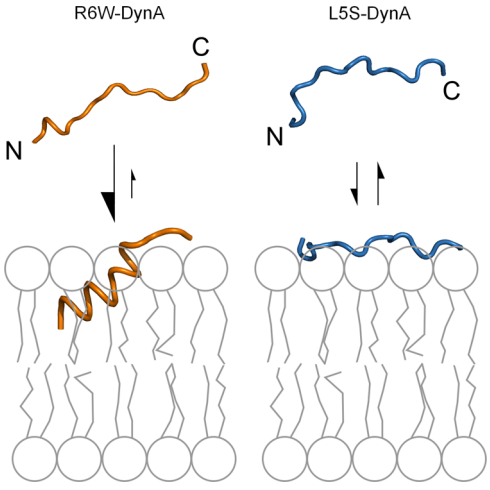

Figure 6. Cartoon representation of the direct membrane interaction of R6W-DynA (left) and L5S-DynA (right). L5S-DynA is mainly unstructured in both buffer and bicelles, and the fractions of bicelle-associated and free peptide are similar in magnitude. The conformational ensemble of R6W-DynA contains a fraction of helical structure in buffer, and this fraction increases in the presence of bicelles. The equilibrium between bicelle-associated and free peptide is displaced toward the bound form.

In contrast, L5S-DynA appears to reside some distance from the lipid chain region, but with its amide protons still somewhat protected from the solvent, except for the very C-terminal residues. This points toward a peptide adopting a rather shallow position in the bicelle (Figure 2). Hence, the Leu5 to Ser replacement causes a weaker bicelle interaction and positions the peptide away from the interior.

The first four amino acid residues in wtDynA and the variants considered here are identical to enkephalin, an endogeneous opioid that interacts with several receptors. A structural study of the five-residue peptide Met-enkephalin in bicelle membrane mimetics similar to those used in the study presented here indicated that this short peptide adopts several conformations, with around 60% of the peptide being bound to bicelles.[70] Here we observe that a larger fraction (90−100%) of the 17-residue peptide R6W-DynA is bound to the bicelles and that there is evidence that the peptide is loosely structured along most of the sequence, indicating a different type of interaction than for Met-enkephalin. Such differences in membrane interactions may explain also differences in the interactions with receptors, as the membrane-bound state of the opioid peptide may have an influence on the affinity for a receptor.[41]

Using the Wimley−White hydrophobicity scale,[71] the net differences in free energy between having the side chains in a membrane and in water were estimated for all three peptides and are summarized in Table 1. These values do not include the cost of partitioning the backbone and should not be overinterpreted but suggest that the R6W variant is more prone to interacting with a bilayer than wtDynA, which in turn is more hydrophobic than L5S. Here we observe that while wtDynA and the R6W variant have the same affinity for the bicelle, they are inserted into the bicelle in somewhat different ways, a result that fits well with the prediction. The corresponding numbers for the N-terminal half of the peptides show a gain in free energy when moving the side chains of wtDynA and R6W-DynA from water to bilayer, but a cost in energy for L5S. Overall, wtDynA and R6W-DynA behave in fairly similar ways, while L5S-DynA is clearly different. A model of how the two variants interact with bicelles is shown in Figure 5. The very clear differences in how the two interact with bicelles can most likely explain the varying toxicity and membrane-perturbing properties observed earlier. R6W-DynA is more toxic and causes membrane perturbations, which can be correlated with the insertion of the peptide into the bilayer. L5S-DynA, on the other hand, appears to be even less toxic than wtDynA and causes no membrane disruption,[40] which in our study is explained by a weak membrane interaction with the bilayer surface.

From a physiological perspective, one should note that DynA belongs to the typical opioid peptides, derived from either of the three precursors, pro-enkephalin, pro-opioimelanocortin, and pro-dynorphin, all sharing the same N-terminal tetrapeptide (Tyr-Gly-Gly-Phe).[72] Chavkin et al. described this segment of the dynorphin peptides as the "message" region, due to this being "the shortest fragment with typical naloxone-reversible opioid activity."[4] Both DynA variants discussed here are the result of mutations in the remaining part of the peptide, the "address" region, responsible for the potency and specificity of DynA. Position 5 has additional significance, because this residue is either Leu or Met in all typical opioid peptides. A study by Turcotte et al.[73] showed that the L5A mutation decreased the potency of DynA(1−13) by ∼95% in two biological assays, while the same mutation of R6 had similar effects on the potency in one assay but a much weaker effect in the other. Similar results were obtained by Snyder et al. for the replacement of R6 with the nonbasic Lys(Ac), and this group also reported a large decrease in KOR selectivity for this mutation.[33] A decrease in potency and selectivity was also the result of replacement of R6 with an Nle residue in DynA(1−

dx.doi.org/10.1021/bi4004205 | *Biochemistry* 2013, 52, 4157−4167

10).[74] A recent study reported nociceptive activity for both L5S- and R6W-DynA when they were intrathecally administered to mice,[75] with the latter peptide being the most potent.

It is interesting to speculate about how the results observed here may be linked to these physiological observations. For both peptide variants, the level of production is considerably increased in the mutant-affected humans, possibly because of a partly corrupted receptor interaction because both variants involve residues close to the crucial N-terminal peptide. For the R6W-DynA variant, the membrane interaction, most likely even stronger than for wtDynA, could be a major part of the explanation for the observed toxicity associated with this variant, both in mutant-affected humans and in the experimental mouse studies.[38,75] For the L5S-DynA variant, the much weaker membrane interaction suggests that other reasons for the link to disease and animal toxicity should be considered, possibly in this case linked to deficient receptor interactions, because of the proximity of the mutation to the N-terminal tetrapeptide.

In conclusion, our results show that the two DynA variants have radically different properties. R6W-DynA shows a strong association with and partial penetration into the phospholipid bicelles, correlated with an increase in structural propensity when transferred from buffer to the lipid bilayer environment. L5S-DynA, on the other hand, is overall unstructured, shows weaker association with the bicelles, and adapts a shallow position in the headgroup region of the bilayer. Our results demonstrate that the direct membrane effects shown by the two variants can most likely be explained by these differences in lipid interactions. Although both sequences have been implicated in disease, the reasons behind this may be different for the two. While direct membrane effects appear to be important for R6W-DynA, the L5S replacement is most likely instead related to a change in receptor interaction.

AUTHOR INFORMATION

Corresponding Author

*E-mail: lena.maler@dbb.su.se. Phone: +46 8 162448. Fax: +46 8 155597.

Funding

This work was supported by grants from the Swedish Research Council, the Knut and Alice Wallenberg Foundation, and the Magnus Bergvall Foundation.

Notes

The authors declare no competing financial interest.

ABBREVIATIONS

5-DOXYL-POPC, 1-palmitoyl-2-stearoyl(5-doxyl)-*sn*-glycero-3-phosphocholine; CD, circular dichroism; DHPC, 1,2-dihexanoyl-d_{22}-*sn*-glycero-3-phosphocholine; DMPC, 1,2-dimyristoyl-*sn*-glycero-3-phosphocholine; DMPG, 1,2-dimyristoyl-*sn*-glycero-3-phospho(1′-*rac*-glycerol); DynA, dynorphin A; DynB, dynorphin B; KOR, κ-opioid receptor; NMR, nuclear magnetic resonance; PDYN, prodynorphin; PRE, paramagnetic relaxation enhancement; SCA23, spinocerebellar ataxia 23.

REFERENCES

(1) Teschemacher, H., Opheim, K. E., Cox, B. M., and Goldstein, A. (1975) A peptide-like substance from pituitary that acts like morphine. I. Isolation. *Life Sci. 16*, 1771−1775.

(2) Goldstein, A., Tachibana, S., Lowney, L., Hunkapiller, M., and Hood, L. (1979) Dynorphin-(1−13), an extraordinarily potent opioid peptide. *Proc. Natl. Acad. Sci. U.S.A. 76*, 6666−6670.

(3) Chavkin, C., and Goldstein, A. (1981) Demonstration of a specific dynorphin receptor in guinea pig ileum myenteric plexus. *Nature 291*, 591−593.

(4) Chavkin, C., and Goldstein, A. (1981) Specific receptor for the opioid peptide dynorphin: Structure−activity relationships. *Proc. Natl. Acad. Sci. U.S.A. 78*, 6543−6547.

(5) Chavkin, C., James, I. F., and Goldstein, A. (1982) Dynorphin is a specific endogenous ligand of the kappa opioid receptor. *Science 215*, 413−415.

(6) Oka, T., Negishi, K., Suda, M., Sawa, A., Fujino, M., and Wakimasu, M. (1982) Evidence that dynorphin-(1−13) acts as an agonist on opioid κ-receptors. *Eur. J. Pharmacol. 77*, 137−141.

(7) Kakidani, H., Furutani, Y., Takahashi, H., Noda, M., Morimoto, Y., Hirose, T., Asai, M., Inayama, S., Nakanishi, S., and Numa, S. (1982) Cloning and sequence analysis of cDNA for porcine β-neo-endorphin/dynorphin precursor. *Nature 298*, 245−249.

(8) Bakalkin, G. Y., Rakhmaninova, A. B., Akparov, V. K., Volodin, A. A., Ovchinnikov, V. V., and Sarkisyan, R. A. (1991) Amino acid sequence pattern in the regulatory peptides. *Int. J. Pept. Protein Res. 38*, 505−510.

(9) Wen, H. L., Mehal, Z. D., Ong, B. H., and Ho, W. K. (1987) Treatment of pain in cancer patients by intrathecal administration of dynorphin. *Peptides 8*, 191−193.

(10) Wen, H. L., Mehal, Z. D., Ong, B. H., Ho, W. K. K., and Wen, D. Y. K. (1985) Intrathecal administration of β-endorphin and dynorphin-(1−13) for the treatment of intractable pain. *Life Sci. 37*, 1213−1220.

(11) Bruchas, M. R., Land, B. B., and Chavkin, C. (2010) The dynorphin/kappa opioid system as a modulator of stress-induced and pro-addictive behaviors. *Brain Res. 1314*, 44−55.

(12) Bruijnzeel, A. W. (2009) Kappa-opioid receptor signaling and brain reward function. *Brain Res. Rev. 62*, 127−146.

(13) Tejeda, H. A., Shippenberg, T. S., and Henriksson, R. (2012) The dynorphin/κ-opioid receptor system and its role in psychiatric disorders. *Cell. Mol. Life Sci. 69*, 857−896.

(14) Bakshi, R., and Faden, A. I. (1990) Competitive and non-competitive NMDA antagonists limit dynorphin A-induced rat hindlimb paralysis. *Brain Res. 507*, 1−5.

(15) Walker, J. (1982) Nonopiate effects of dynorphin and des-tyr-dynorphin. *Science 218*, 1136−1138.

(16) Tan-No, K., Cebers, G., Yakovleva, T., Goh, B. H., Gileva, I., Reznikov, K., Aguilar-Santelises, M., Hauser, K. F., Terenius, L., and Bakalkin, G. (2001) Cytotoxic effects of dynorphins through nonopioid intracellular mechanisms. *Exp. Cell Res. 269*, 54−63.

(17) Marinova, Z., Vukojevic, V., Surcheva, S., Yakovleva, T., Cebers, G., Pasikova, N., Usynin, I., Hugonin, L., Fang, W., Hallberg, M., Hirschberg, D., Bergman, T., Langel, U., Hauser, K. F., Pramanik, A., Aldrich, J. V., Gräslund, A., Terenius, L., and Bakalkin, G. (2005) Translocation of dynorphin neuropeptides across the plasma membrane. A putative mechanism of signal transmission. *J. Biol. Chem. 280*, 26360−26370.

(18) Hugonin, L., Vukojević, V., Bakalkin, G., and Gräslund, A. (2006) Membrane leakage induced by dynorphins. *FEBS Lett. 580*, 3201−3205.

(19) Naito, A., Nagao, T., Obata, M., Shindo, Y., Okamoto, M., Yokoyama, S., Tuzi, S., and Saitô, H. (2002) Dynorphin induced magnetic ordering in lipid bilayers as studied by ^{31}P NMR spectroscopy. *Biochim. Biophys. Acta 1158*, 34−44.

(20) Naqvi, T., Haq, W., and Mathur, K. B. (1998) Structure-activity relationship studies of dynorphin A and related peptides. *Peptides 19*, 1277−1292.

(21) Lung, F. T., Chen, C., and Liu, J. (2005) Development of highly potent and selective dynorphin A analogues as new medicines. *J. Pept. Res. 66*, 263−276.

(22) Arttamangkul, S., Ishmael, J. E., Murray, T. F., Grandy, D. K., DeLander, G. E., Kieffer, B. L., and Aldrich, J. V. (1997) Synthesis and opioid activity of conformationally constrained dynorphin A analogues. 2. Conformational constraint in the "address" sequence. *J. Med. Chem. 40*, 1211−1218.

(23) Arttamangkul, S., Murray, T. F., DeLander, G. E., and Aldrich, J. V. (1995) Synthesis and opioid activity of conformationally constrained dynorphin A analogues. 1. Conformational constraint in the "message" sequence. *J. Med. Chem. 38*, 2410−2417.
(24) Choi, H., Murray, T. F., DeLander, G. E., Caldwell, V., and Aldrich, J. V. (1992) N-Terminal alkylated derivatives of [D-Pro10]dynorphin A-(1−11) are highly selective for κ-opioid receptors. *J. Med. Chem. 35*, 4638−4639.
(25) Choi, H., Murray, T. F., DeLander, G. E., Schmidt, W. K., and Aldrich, J. V. (1997) Synthesis and opioid activity of [D-Pro10]-dynorphin A-(1−11) analogues with N-terminal alkyl substitution. *J. Med. Chem. 40*, 2733−2739.
(26) Fang, W., Cui, Y., Murray, T. F., and Aldrich, J. V. (2009) Design, synthesis, and pharmacological activities of dynorphin A analogues cyclized by ring-closing metathesis. *J. Med. Chem. 52*, 5619−5625.
(27) Gairin, J. E., Mazarguil, H., Alvinerie, P., Saint-Pierre, S., Meunier, J. C., and Cros, J. (1986) Synthesis and biological activities of dynorphin A analogues with opioid antagonist properties. *J. Med. Chem. 29*, 1913−1917.
(28) Lapalu, S., Moisand, C., Mazarguil, H., Cambois, G., Mollereau, C., and Meunier, J. C. (1997) Comparison of the structure-activity relationships of nociceptin and dynorphin A using chimeric peptides. *FEBS Lett. 417*, 333−336.
(29) Lemaire, S., Lafrance, L., and Dumont, M. (1986) Synthesis and biological activity of dynorphin-(1−13) and analogs substituted in positions 8 and 10. *Int. J. Pept. Protein Res. 27*, 300−305.
(30) Lung, F. D., Collins, N., Stropova, D., Davis, P., Yamamura, H. I., Porreca, F., and Hruby, V. J. (1996) Design, synthesis, and biological activities of cyclic lactam peptide analogues of dynorphin A(1−11)-NH2. *J. Med. Chem. 39*, 1136−1141.
(31) Meyer, J. P., Collins, N., Lung, F. D., Davis, P., Zalewska, T., Porreca, F., Yamamura, H. I., and Hruby, V. J. (1994) Design, synthesis, and biological properties of highly potent cyclic dynorphin A analogues. Analogues cyclized between positions 5 and 11. *J. Med. Chem. 37*, 3910−3917.
(32) Patkar, K. A., Murray, T. F., and Aldrich, J. V. (2009) The effects of C-terminal modifications on the opioid activity of [N-BenzylTyr1]-dynorphin A-(1−11) analogues. *J. Med. Chem. 52*, 6814−6821.
(33) Snyder, K. R., Story, S. C., Heidt, M. E., Murray, T. F., DeLander, G. E., and Aldrich, J. V. (1992) Effect of modification of the basic residues of dynorphin A-(1−13) amide on kappa opioid receptor selectivity and opioid activity. *J. Med. Chem. 35*, 4330−4333.
(34) Vig, B. S., Murray, T. F., and Aldrich, J. V. (2004) Synthesis and opioid activity of side-chain-to-side-chain cyclic dynorphin A-(1−11) amide analogues cyclized between positions 2 and 5. 1. Substitutions in position 3. *J. Med. Chem. 47*, 446−455.
(35) Vig, B. S., Murray, T. F., and Aldrich, J. V. (2003) A novel N-terminal cyclic dynorphin A analogue *cyclo*^{N,5}[Trp^3,Trp^4,Glu^5] dynorphin A-(1−11)NH_2 that lacks the basic N-terminus. *J. Med. Chem. 46*, 1279−1282.
(36) Yoshino, H., Nakazawa, T., Arakawa, Y., Kaneko, T., Tsuchiya, Y., Matsunaga, M., Araki, S., Ikeda, M., Yamatsu, K., and Tachibana, S. (1990) Synthesis and structure-activity relationships of dynorphin A-(1−8) amide analogues. *J. Med. Chem. 33*, 206−212.
(37) Wu, H., Wacker, D., Mileni, M., Katritch, V., Han, G. W., Vardy, E., Liu, W., Thompson, A. A., Huang, X., Carroll, F. I., Mascarella, S. W., Westkaemper, R. B., Mosier, P. D., Roth, B. L., Cherezov, V., and Stevens, R. C. (2012) Structure of the human κ-opioid receptor in complex with JDTic. *Nature 485*, 327−332.
(38) Bakalkin, G., Watanabe, H., Jezierska, J., Depoorter, C., Verschuuren-Bemelmans, C., Bazov, I., Artemenko, K. A., Yakovleva, T., Dooijes, D., and Van de Warrenburg, B. P. C. (2010) Prodynorphin mutations cause the neurodegenerative disorder spinocerebellar ataxia type 23. *Am. J. Hum. Genet. 87*, 593−603.
(39) Jezierska, J., Stevanin, G., Watanabe, H., Fokkens, M. R., Zagnoli, F., Kok, J., Goas, J., Bertrand, P., Robin, C., Brice, A., Bakalkin, G., Durr, A., and Verbeek, D. S. (2013) Identification and characterization of novel PDYN mutations in dominant cerebellar ataxia cases. *J. Neurol.*, DOI: 10.1007/s00415-013-6882-6.
(40) Madani, F., Taqi, M. M., Wärmländer, S. K. T. S., Verbeek, D. S., Bakalkin, G., and Gräslund, A. (2011) Perturbations of model membranes induced by pathogenic dynorphin A mutants causing neurodegeneration in human brain. *Biochem. Biophys. Res. Commun. 411*, 111−114.
(41) Sargent, D. F., and Schwyzer, R. (1986) Membrane lipid phase as catalyst for peptide-receptor interactions. *Proc. Natl. Acad. Sci. U.S.A. 83*, 5774−5778.
(42) Alford, D. R., Renugopalakrishnan, V., and Duzgunes, N. (1996) Dynorphin-phospholipid membrane interactions: Role of phospholipid head-group and cholesterol. *Int. J. Pept. Protein Res. 47*, 84−90.
(43) Hugonin, L., Barth, A., Gräslund, A., and Perálvarez-Marín, A. (2008) Secondary structure transitions and aggregation induced in dynorphin neuropeptides by the detergent sodium dodecyl sulfate. *Biochim. Biophys. Acta 1778*, 2580−2587.
(44) Lind, J., Gräslund, A., and Mäler, L. (2006) Membrane interactions of dynorphins. *Biochemistry 45*, 15931−15940.
(45) Schwyzer, R. (1986) Estimated conformation, orientation, and accumulation of dynorphin A-(1−13)-tridecapeptide on the surface of neutral lipid membranes. *Biochemistry 25*, 4281−4286.
(46) Glover, K. J., Whiles, J. A., Wu, G., jun Yu, N., Deems, R., Struppe, J. O., Stark, R. E., Komives, E. A., and Vold, R. R. (2001) Structural evaluation of phospholipid bicelles for solution-state studies of membrane-associated biomolecules. *Biophys. J. 81*, 2163−2171.
(47) Vold, R., Prosser, R. S., and Deese, A. (1997) Isotropic solutions of phospholipid bicelles: A new membrane mimetic for high-resolution NMR studies of polypeptides. *J. Biomol. NMR 9*, 329−335.
(48) Svennerholm, L. (1968) Distribution and fatty acid composition of phosphoglycerides in normal human brain. *J. Lipid Res. 9*, 570−579.
(49) Mäler, L., and Gräslund, A. (2011) NMR Studies of Three-Dimensional Structure and Positioning of CPPs in Membrane Model Systems. *Methods Mol. Biol. 683*, 57−67.
(50) Louis-Jeune, C., Andrade-Navarro, M., and Perez-Iratxeta, C. (2012) Prediction of protein secondary structure from circular dichroism using theoretically derived spectra. *Proteins 80*, 374−381.
(51) Delaglio, F., Grzesiek, S., Vuister, G. W., Zhu, G., Pfeifer, J., and Bax, A. (1995) NMRPipe: A multidimensional spectral processing system based on UNIX pipes. *J. Biomol. NMR 6*, 277−293.
(52) Goddard, T. D., and Kneller, D. G. (2006) *Sparky 3*, University of California, San Francisco.
(53) Vogel, A., Scheidt, H. A., and Huster, D. (2003) The distribution of lipid attached spin probes in bilayers: Application to membrane protein topology. *Biophys. J. 85*, 1691−1701.
(54) Callaghan, P. T., Komlosh, M. E., and Nyden, M. (1998) High magnetic field gradient PGSE NMR in the presence of a large polarizing field. *J. Magn. Reson. 133*, 177−182.
(55) Stejskal, E. O., and Tanner, J. E. (1965) Spin diffusion measurements: Spin echoes in the presence of a time-dependent field gradient. *J. Chem. Phys. 42*, 288−288.
(56) von Meerwall, E., and Kamat, M. (1989) Effect of residual field gradients on pulsed-gradient NMR diffusion measurements. *J. Magn. Reson. 83*, 309−323.
(57) Longsworth, L. (1960) The mutual diffusion of light and heavy water. *J. Phys. Chem. 64*, 1914−1917.
(58) van Dam, L., Karlsson, G., and Edwards, K. (2004) Direct observation and characterization of DMPC/DHPC aggregates under conditions relevant for biological solution NMR. *Biochim. Biophys. Acta 1664*, 241−256.
(59) Triba, M. N., Warschawski, D. E., and Devaux, P. F. (2005) Reinvestigation by phosphorus NMR of lipid distribution in bicelles. *Biophys. J. 88*, 1887−1901.
(60) Chou, J. J., Kaufman, J. D., Stahl, S. J., Wingfield, P. T., and Bax, A. (2002) Micelle-induced curvature in a water-insoluble HIV-1 Env peptide revealed by NMR dipolar coupling measurement in a stretched polyacrylamide gel. *J. Am. Chem. Soc. 124*, 2450−2451.

(61) Andersson, A., and Mäler, L. (2005) Magnetic resonance investigations of lipid motion in isotropic bicelles. *Langmuir 21*, 7702−7709.
(62) Wishart, D., Bigam, C., Holm, A., Hodges, R., and Sykes, B. (1995) ^{1}H, ^{13}C and ^{15}N random coil NMR chemical shifts of the common amino acids. I. Investigations of nearest-neighbor effects. *J. Biomol. NMR 5*, 67−81.
(63) Marsh, J. A., Singh, V. K., Jia, Z., and Forman-Kay, J. (2006) Sensitivity of secondary structure propensities to sequence differences between α- and γ-synuclein: Implications for fibrillation. *Protein Sci. 15*, 2795−2804.
(64) Perczel, A., Lengyel, I., Mantsch, H. H., and Fasman, G. D. (1993) Analysis of hydrogen bonds in peptides, based on the hydration affinity of amides. *J. Mol. Struct. 297*, 115−126.
(65) Zhou, N. E., Zhu, B. Y., Sykes, B. D., and Hodges, R. S. (1992) Relationship between amide proton chemical shifts and hydrogen bonding in amphipathic α-helical peptides. *J. Am. Chem. Soc. 114*, 4320−4326.
(66) Sankararamakrishnan, R., and Weinstein, H. (2000) Molecular dynamics simulations predict a tilted orientation for the helical region of dynorphin A(1−17) in dimyristoylphosphatidylcholine bilayers. *Biophys. J. 79*, 2331−2344.
(67) de Planque, M. R., Kruijtzer, J. A., Liskamp, R. M., Marsh, D., Greathouse, D. V., Koeppe, R. E., II, de Kruijff, B., and Killian, J. A. (1999) Different membrane anchoring positions of tryptophan and lysine in synthetic transmembrane α-helical peptides. *J. Biol. Chem. 274*, 20839−20846.
(68) Killian, J. A., and von Heijne, G. (2000) How proteins adapt to a membrane-water interface. *Trends Biochem. Sci. 25*, 429−434.
(69) Uezono, T., Toraya, S., Obata, M., Nishimura, K., Tuzi, S., Saitô, H., and Naito, A. (2005) Structure and orientation of dynorphin bound to lipid bilayers by ^{13}C solid-state NMR. *J. Mol. Struct. 749*, 13−19.
(70) Marcotte, I., Separovic, F., Auger, M., and Gagné, S. (2004) A multidimensional ^{1}H NMR investigation of the conformation of methionine-enkephalin in fast-tumbling bicelles. *Biophys. J. 86*, 1587−1600.
(71) Wimley, W. C., and White, S. H. (1996) Experimentally determined hydrophobicity scale for proteins at membrane interfaces. *Nat. Struct. Biol. 3*, 842−848.
(72) Janecka, A., Fichna, J., and Janecki, T. (2004) Opioid receptors and their ligands. *Curr. Top. Med. Chem. 4*, 1−17.
(73) Turcotte, A., Lalonde, J., St-Pierre, S., and Lemaire, S. (1984) Dynorphin-(1−13). I. Structure-function relationships of Ala-containing analogs. *Int. J. Pept. Protein Res. 23*, 361−367.
(74) Kawasaki, A. M., Knapp, R. J., Walton, A., Wire, W. S., Zalewska, T., Yamamura, H. I., Porreca, F., Burks, T. F., and Hruby, V. J. (1993) Syntheses, opioid binding affinities, and potencies of dynorphin A analogues substituted in positions, 1, 6, 7, 8 and 10. *Int. J. Pept. Protein Res. 42*, 411−419.
(75) Watanabe, H., Mizoguchi, H., Verbeek, D. S., Kuzmin, A., Nyberg, F., Krishtal, O., Sakurada, S., and Bakalkin, G. (2012) Non-opioid nociceptive activity of human dynorphin mutants that cause neurodegenerative disorder spinocerebellar ataxia type 23. *Peptides 35*, 306−310.